crystals

MDPI

Article

Sustainable Gypsum Composites with Recycled Plasterboard Aggregates and Metakaolin Waste: Hydration, Microstructure and Acoustic Performance

Danutė Vaičiukynienė [1,*], Dalia Nizevičienė [2], Jūratė Mockienė [3], Vilimantas Vaičiukynas [3] and Laura Vitola [1,4]

[1] Faculty of Architecture and Civil Engineering, Kaunas University of Technology, Studentų St. 48, LT-51367 Kaunas, Lithuania; laura.vitola_1@rtu.lv
[2] Faculty of Electrical and Electronics Engineering, Kaunas University of Technology, Studentų St. 48, LT-51367 Kaunas, Lithuania; dalia.nizeviciene@ktu.lt
[3] Faculty of Industrial Engineering and Technology, Lietuvos Inzinerijos Kolegija Higher Education Institution, Tvirtovės al. 35, LT-50155 Kaunas, Lithuania; jurate.moskiene@lik.tech (J.M.); vilimantas.vaiciukynas@lik.tech (V.V.)
[4] Institute of Sustainable Building Materials and Engineering Systems, Riga Technical University, Kipsalas 6A, LV-1048 Riga, Latvia
* Correspondence: danute.vaiciukyniene@ktu.lt

Abstract

This study examines gypsum-based matrix composites reinforced with recycled gypsum plasterboard aggregates (RGPAs) and metakaolin waste (MKW) from expanded glass granule production. The study addresses the current lack of research on the combined use of RGPAs and MKW within a single gypsum matrix, providing new insight into their interaction and the potential of MKW to counterbalance RGPA-induced heterogeneity. The results show that RGPAs accelerate dihydrate nucleation, while MKW prolongs hydration through water adsorption, producing a more controlled thermal profile. MKW also enhances composite durability, allowing for the materials to retain a greater proportion of their strength after water exposure. XRD and SEM analyses confirm that MKW refines crystal morphology and enhances microstructural stability, whereas RGPAs increase porosity and heterogeneity. MKW further modifies the hydration pathway by slowing hemihydrate dissolution and delaying dihydrate precipitation, while RGPAs contribute inert mineral phases without participating in hydration. Gypsum dihydrate remains the dominant phase in all composites, but MKW-containing mixtures exhibit partial retention of bassanite, confirming its influence on hydration kinetics. Acoustic tests demonstrate that all composites reduce noise by 8.5–10.5 dBA, with 90BGMK achieving the lowest sound pressure level (82 dBA) and strongest high-frequency attenuation. Overall, MKW effectively compensates for RGPA-induced heterogeneity, enabling the development of sustainable, mechanically robust, and acoustically efficient gypsum composites aligned with circular economy principles.

Keywords: sustainable building materials; gypsum recycling; metakaolin waste utilization; hemihydrate hydration behavior; sound insulation

Check for updates

Academic Editor: Leonid M. Kustov

Received: 27 August 2026
Revised: 23 September 2026
Accepted: 27 September 2026
Published: 30 September 2026

Copyright: © 2026 by the authors. Licensee MDPI, Basel, Switzerland. This article is an open access article distributed under the terms and conditions of the Creative Commons Attribution (CC BY) license.

1. Introduction

Gypsum and gypsum-based products are widely used in the construction sector, resulting in large amounts of waste, including plasterboard offcuts generated during new construction and used boards arising from demolition works. Overall, the studies show that gypsum waste can be repeatedly recycled into strong, high-quality products—including plaster, boards, and even 3D-printing materials—while keeping good mechanical performance

and reducing environmental impact. Alongside performance improvements, life-cycle studies highlight the environmental benefits of recycling gypsum. Recycled gypsum often has lower environmental impacts than natural, particularly in land use and resource depletion categories, although transport distance remains a key factor [1]. Erbs et al. [2] found that plasterboard sheets, composed of a gypsum core and paper liners, can be fully recycled, with waste-based boards achieving a surface mass of 11.20 kg/m^2, flexural strength of 3.09/2.62 MPa, and compressive strength of 14.37 MPa. The study showed that it is technically feasible to manufacture plasterboards entirely from waste materials without losing the required mechanical performance. The study [3] established that heating plasterboard waste at 150 °C for 3 h fully converts gypsum into basanite, eliminating shrinkage issues and producing recycled plasters with excellent mechanical performance, including a compressive strength of 8.40 MPa, which exceeds commercial gypsum by 38.7%. Ma et al. [4] stated that a high value-added recycling route was developed in which waste gypsum board is converted into high-precision 3D-printing α-hemihydrate powder, optimized using 0.05 wt.% sodium succinate at pH 5 to produce crystals with an aspect ratio of 1.07 and a length of about 10 μm. The resulting recycled α-hemihydrate achieved a mechanical strength of 25.5 MPa and enabled accurate 3D printing, demonstrating strong potential for industrial upcycling of waste gypsum. Finally, multi-cycle recycling studies confirm that gypsum plaster waste can be recycled repeatedly—after 1, 3, and 5 cycles—without altering chemical composition or crystalline phases, while maintaining good mechanical performance, demonstrating that multi-cycle recycling is technically feasible, low-energy, and suitable for producing new building components with reduced environmental impact [5]. However, previous studies have also shown that the recycling of gypsum and its reconversion into hemihydrate may lead to shorter setting times as a result of changes in crystal morphology and increased nucleation activity. Therefore, even when the mechanical properties of recycled gypsum products are preserved, accelerated setting can create practical challenges during mixing, processing, transportation, and on-site application, which should be considered when developing recycled gypsum-based materials.

Recent studies show that the properties of gypsum composites can be significantly improved by adjusting their microstructure—for example, by adding mineral modifiers, choosing suitable matrix–filler density ratios, using porous or waste-based fillers, fire-resistant additives, or heat-treated lightweight aggregates. These modifications can increase strength, lower density and thermal conductivity, and in some cases also improve acoustic and fire-resistant performance. Studies consistently show that the performance of gypsum composites can be greatly improved by deliberately modifying their microstructure. Study [6] found that mineral modifying ($Al_2(SO_4)_3 \cdot 18H_2O$.) complexes strengthen the material by changing the shape of gypsum crystals and creating a denser, more crack-resistant structure, which allows these composites to outperform unmodified mixes and makes them suitable for high-strength applications. Vimmrova et al. [7] further showed that the most effective approach for producing lightweight gypsum materials is combining a higher-density gypsum matrix with low-density fillers, as evidenced by the mix with 5% expanded perlite, which achieved a bulk density of 547 kg/m^3, thermal conductivity of 0.12 W/m·K, and compressive strength of 2.0 MPa, whereas foamed gypsum with denser aggregates provided good thermal insulation but insufficient mechanical strength. Complementary findings [8] reveal that porous fillers promote denser crystal packing and improved strength, with expanded clay composites reaching 12.5 MPa while retaining only 20% of the reference thermal conductivity, and polyurethane foam composites achieving the lowest strength (2.9 MPa) but the best insulation (0.211 W/m·K). Another study [9] demonstrated that hybrid waste-based fillers—paper, polystyrene, and polyester—can reduce bulk density by 33%, lower thermal conductivity to 0.13–0.18 W/m·K, increase flexural strength by 42%,

and maintain compressive strength above 2 MPa, while also improving ductility and fire resistance. Wang et al. [10] showed that adding 0–30 wt.% palygorskite and 0.5 wt.% glass fibre produces lightweight, fire-resistant gypsum boards whose density decreases from 1059 to 795 kg/m^3, whose ambient-side temperature during a 90 min fire test is reduced by 150 °C, and which retain 0.15 MPa post-fire strength due to fibre bridging and palygorskite sintering. Finally, Argalis et al. [11] demonstrated that heat-treated EPS fillers (40–100 kg/m^3) enable the production of ultra-light gypsum composites with densities of 48–194 kg/m^3, compressive strength of 15–136 kPa, thermal conductivity of 0.0390–0.0604 W/(mK), and excellent sound absorption reaching 0.88 at 600–800 Hz.

Numerous studies indicate that aluminosilicate additives such as metakaolin can significantly improve the mechanical and functional performance of various gypsum composites. Kishor et al. [12] demonstrated that glass-cullet-modified mortar supplemented with metakaolin and flue gas desulfurization gypsum exhibits a synergistic response: metakaolin enhances pozzolanic reactivity and C–S–H formation, while the gypsum regulates hydration through controlled ettringite generation, effectively compensating for the strength reduction caused by the inert nature of glass particles. Yildizel et al. [13] reported that incorporating metakaolin improved the drying (shrinkage) behavior of gypsum-based composites and reduced the risk of early crack formation, while also enhancing their strength and durability. Moradi et al. [14] highlighted that metakaolin influences the hydration process and microstructure of gypsum, with its dosage playing a key role in shaping these effects. Their experimental results showed that metakaolin enhances the physical and mechanical performance of gypsum by filling interstitial pores and increasing resistance to fracture. Overall, the study suggests that gypsum–metakaolin composites hold strong potential for lightweight, porous building applications. Another study [15] revealed that replacing 2.5–7.5% of gypsum with metakaolin slightly increased compressive strength (from 12.36 MPa to 13.11 MPa), while a minor rise in density and water absorption led to increased porosity in the gypsum composites.

Although many studies show that gypsum waste can be successfully recycled into new products and that metakaolin together with lightweight fillers can enhance the microstructure and mechanical performance of gypsum composites, there is still a lack of systematic research examining the combined effect of recycled gypsum plasterboard aggregates (RGPAs) and metakaolin waste (MKW) within a single gypsum matrix. Existing studies investigate these additives separately, leaving unclear how RGPAs and MKW interact, how their combination influences composite structure, strength, density, porosity, and acoustic performance, and whether MKW can compensate for the strength reduction typically caused by recycled aggregates. Furthermore, the literature provides almost no insight into the use of metakaolin waste derived from expanded glass granule production, despite its potential value in circular economy applications. Consequently, it remains unknown whether the combination of RGPAs and MKW can produce high-quality, mechanically robust, and sustainable gypsum composites.

The aim of this study is to evaluate the effects of RGPAs and MKW from expanded glass granule production on the mechanical, physical, and functional properties of gypsum composites, with a focus on understanding their interaction and potential to improve composite strength, density, and acoustic characteristics. The study seeks to identify optimal the RGPA amount that enable the development of sustainable, high-performance gypsum composites suitable for construction applications and aligned with circular economy principles.

2. Materials and Methods

2.1. Characterization of Initial Materials

The chemical composition of the initial materials used for gypsum-based matrix composites is presented in Table 1. Commercial building gypsum (BG) is dominated by CaO (36,1%) and SO_3 (43,3%), which is typical for construction-grade calcium sulphate hemihydrate. Smaller quantities of SiO_2, Al_2O_3, MgO and alkali oxides indicate minor mineral impurities originating from raw gypsum sources.

Table 1. Chemical composition according to XRF of initial materials for gypsum-based matrix composites, wt.%.

Oxides	CaO	MgO	SO_3	Fe_2O_3	Al_2O_3	TiO_2	SiO_2	K_2O	Na_2O	Other	LOI *
BG	36.1	5.60	43.3	-	1.63	-	4.97	0.714	-	0.79	6.90
RGPA	32.8	1.04	37.9	0.43	0.62	0.06	2.64	0.33	-	5.68	18.5
MKW	2.65	0.87	0.14	0.87	30.32	0.53	54.66	0.69	7.06	0.28	1.93

* LOI—loss on ignition.

Recycled gypsum plasterboard aggregates (RGPAs) were obtained from waste plasterboard generated during construction and demolition activities. The waste plasterboard was mechanically crushed and processed to produce granular aggregates for incorporation into gypsum composites. Based on the XRF analysis, RGPAs contain 32.8 wt.% CaO and 37.9 wt.% SO_3, corresponding to approximately 70.7 wt.% $CaSO_4$. When recalculated as calcium sulphate dihydrate ($CaSO_4 \cdot 2H_2O$), the dominant phase in plasterboard gypsum, the content reaches approximately 89.5 wt.%. Therefore, RGPAs consist predominantly of gypsum dihydrate, while the remaining fraction comprises mineral impurities, residual paper fibres, organic matter, and other minor constituents, as reflected by the 18.5 wt.% loss on ignition and 5.68 wt.% of other oxides. These impurities are inherent to recycled plasterboard materials and may contribute to the heterogeneity of the composite microstructure. The paper liners were removed manually prior to crushing; however, small amounts of residual fibres and organic matter remained in the recycled aggregate fraction, as indicated by the chemical composition and loss-on-ignition results.

Metakaolin waste (MKW) shows a distinctly different chemical composition, characteristic of calcined aluminosilicate materials. It is rich in SiO_2 (54.66%) and Al_2O_3 (30.32%), with minor amounts of alkali oxides (Na_2O, K_2O), Fe_2O_3, TiO_2, and very low CaO (2.65%) and SO_3 (0.14%). This composition confirms that MKW is a silica and alumina rich aluminosilicate material that may influence hydration kinetics and microstructure development.

Overall, the data indicate that BG and RGPAs share a calcium-sulfate-dominated chemical structure suitable for gypsum matrix formation, while MKW provides a silica-alumina-rich phase capable of modifying hydration, microstructure, and mechanical performance when incorporated into gypsum composites.

X-ray diffraction (XRD) analysis was employed to determine the mineralogical composition of the raw materials, while scanning electron microscopy (SEM) was used to examine their microstructural features. Building gypsum (BG) (Figure 1a) is predominantly composed of calcium sulfate hemihydrate $CaSO_4 \cdot 0.5H_2O$, identified as bassanite (B), with dolomite (D) present as a minor phase. In contrast, the recycled gypsum plasterboard aggregates (RGPAs) (Figure 1b) are characterized by a dominant calcium sulfate dihydrate $CaSO_4 \cdot 2H_2O$ (gypsum, G), accompanied by impurities of dolomite (D), quartz (Q) and bassanite (B). The metakaolin waste (MKW) (Figure 1c) consists of crystalline aluminosilicate phases, primarily muscovite (M), anorthoclase (An) and quartz (Q).

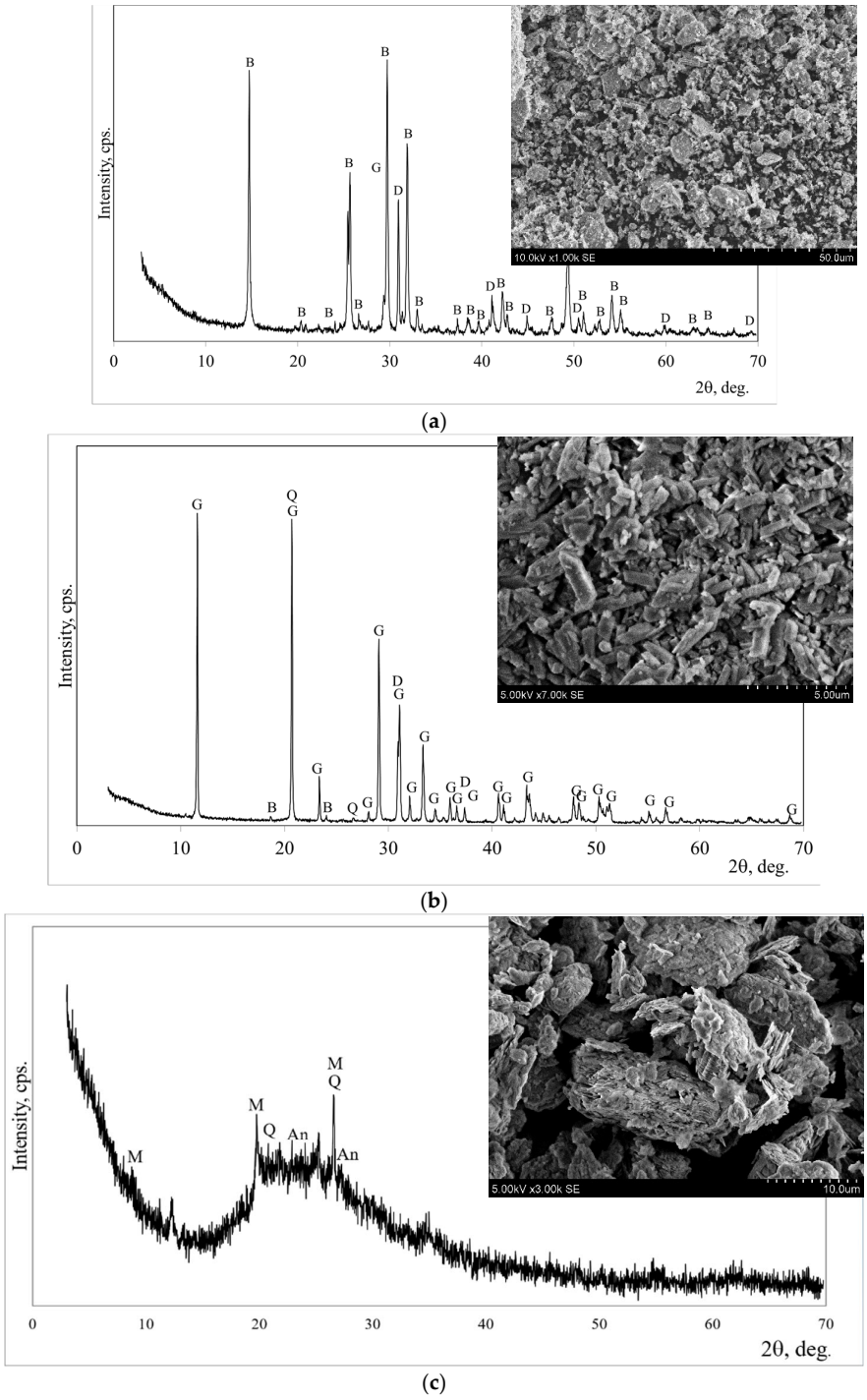


Figure 1. Mineral composition (XRD analysis) and microstructure (SEM analysis) of (**a**) building gypsum, (**b**) recycled gypsum plasterboard aggregates and (**c**) metakaolin waste: G—gypsum $CaSO_4 \cdot 2H_2O$ (33–331), B—basanite $CaSO_4 \cdot 0.5H_2O$ (33–310), D—dolomite $CaMg(CO_3)_2$ (74–1687), Q—quartz SiO_2 (72–916), M—muscovite $(K, Na)(Al, Mg, Fe)_2(Si_{3.1}Al_{0.9})O_{10}(OH)_2$ (pdf No 7–42) and An—anorthoclase $(Na_{0.667}\ K_{0.333})(AlSi_{3O8})$ (pdf No 75–1631).

The SEM micrographs further highlight the distinct microstructural features of the investigated materials. Building gypsum (BG) exhibits a heterogeneous and fragmented microstructure, reflecting the variability inherent to its production and processing. In contrast, recycled gypsum plasterboard aggregates (RGPAs) display typical plate-like gypsum crystal morphologies, characteristic of hydrated calcium sulfate dihydrate formed during the plasterboard manufacturing process. Metakaolin waste (MKW) shows a layered

and angular assemblage of silicate particles, consistent with the crystalline phases identified by XRD and indicative of its aluminosilicate origin.

The dry density of the BG powder is 2.60 g/cm^3, which is comparable to the density of the metakaolin waste powder (2.59 g/cm^3). The dry bulk density of the aggregates prepared from recycled gypsum plasterboard is 581.01 kg/m^3.

As a setting retarder, TARDA (tartaric acid) was incorporated into the gypsum binder systems to prolong the setting time of the paste. In gypsum systems, TARDA is typically used at very low dosages—ranging from 0.02% to approximately 0.20% of the binder mass—depending on the required degree of setting time delay.

2.2. Preparation of the Mixtures

Table 2 presents the formulation of gypsum-based composites prepared in this study, including the proportions of building gypsum (BG), recycled gypsum plasterboard aggregates (RGPAs), metakaolin waste (MKW), and the setting retarder Tarda. In all mixtures, the percentages of BG, RGPAs and MKW are expressed as weight percentages of the total solid mass; RGPAs partially replace the gypsum binder, while MKW is added as an additional aluminosilicate component. The mixtures were designed to evaluate the influence of recycled gypsum and metakaolin waste on the main properties of gypsum composites. The mixtures containing only building gypsum (100–60BG) include increasing amounts of recycled gypsum plasterboard aggregates (RGPAs), from 10 wt.% up to 40 wt.%. This stepwise replacement allows us to evaluate how RGPAs influence the main properties of gypsum-based matrix composites.

Table 2. The composition of initial materials for gypsum composite.

Samples	BG, wt.%	RGPA, wt.%	MKW, wt.%	Retarder, wt.% *	W/G
100BG	100	0	0	0.05	0.41
90BG	90	10	0	0.05	0.41
80BG	80	20	0	0.05	0.41
70BG	70	30	0	0.05	0.42
60BG	60	40	0	0.05	0.42
100BGMK	100	0	10	0.05	0.40
90BGMK	90	10	10	0.05	0.40
80BGMK	80	20	10	0.05	0.41
70BGMK	70	30	10	0.05	0.42
60BGMK	60	40	10	0.05	0.43

* The setting retarder TARDA.

A second mixture group (100–60BGMK) contains a fixed amount of metakaolin waste (10 wt.%) together with different proportions of RGPAs. The use of 10 wt.% metakaolin is consistent with previous research [16], where similar dosages were incorporated into gypsum-based composite systems to enhance microstructure development and mechanical performance. The addition of MKW introduces an amorphous aluminosilicate phase that is expected to influence hydration kinetics and the development of the composite microstructure. The water-to-gypsum ratio (W/G) ranges from 0.40 to 0.43, corresponding to the normal consistency of the prepared pastes.

When mixing the mass for gypsum-based matrix composites, the solid initial materials were first carefully blended in the dry state. After that, the setting retarder was dissolved in the required amount of water. Then, the solution of water and retarder was added to the

solid material mixture and homogenized by mixing for 60 s (Figure 2). The mixing process was carried out using a portable mortar mixer (RUBIMIX-9N, Germans Boada, S.A., Rubí, Spain) at a speed of 780 RPM. After mixing, the samples were molded.

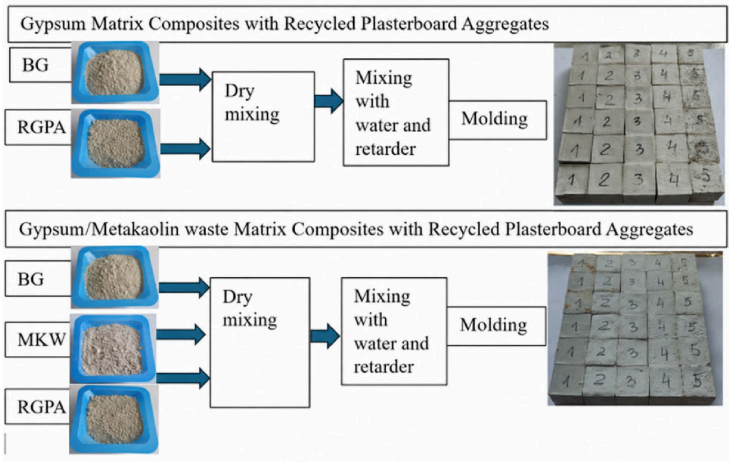


Figure 2. Flow diagram for gypsum-based matrix composites reinforced with recycled gypsum plasterboard aggregates mix preparation.

2.3. Experimental Techniques

The elemental composition of the initial materials was determined via X-ray fluorescence (XRF) analysis, using a Bruker X-ray S8 Tiger WD spectrometer (Bruker AXS GmbH, Karlsruhe, Germany) featuring a rhodium (Rh) tube. The anode voltage was 60 kV, and the electric current intensity was 160 mA. The powder samples were processed in a helium atmosphere. The results were analyzed using the SPECTRA Plus QUANT EXPRESS method.

The mineral composition (XRD) was investigated with the X-ray diffractometer DRON—7 (Bourevestnik, Saint Petersburg, Russia), with a Bragg–Brentano geometry. The device applied Ni-filtered CuKα radiation and a graphite monochromator, using 30 kV voltage and 20 mA emission current. The peaks corresponding to the mineral compounds were identified using the Oxford Cryosystems Crystallographica Search-Match 3.1 software and the PDF-2 database.

A microstructural analysis was performed with a scanning electron microscope, (SEM) Hitachi S-3400N Type II (Hitachi High-Technologies Corporation, Naka, Japan), with image resolutions of secondary electrons in a high vacuum of ≥3 nm (when the potential difference is 30 kV), and ≥10 nm (when it is 3 kV).

The hydration temperature of the cement paste was monitored using a semi-adiabatic calorimetry setup compliant with EN 196-9:2010 [17]. Temperature evolution was captured with an 8-channel USB TC-08 data acquisition unit equipped with a K-type thermocouple, which enables measurements across a wide thermal range (−270 °C to +1820 °C).

In order to determine the mechanical properties of the gypsum-based composites, cubic samples measuring 40 × 40 × 40 mm were prepared from pastes of normal consistency. The water-to-binder ratio corresponding to normal consistency was determined in accordance with EN 196-3 [18]. After casting, the samples were cured under laboratory air conditions for 7 days and subsequently dried at 40 °C until constant mass was reached. Mechanical testing was performed at the age of 7 days using a ToniTechnik 2020.0600/132/02 computer-controlled testing machine (Toni Technik Baustoffprüfsysteme GmbH, Berlin, Germany). The compressive strength of the samples was determined according to EN 13279-2 [19], applying a loading rate of 1 MPa/s. The dry density of hardened gypsum composite specimens incorporating recycled plasterboard aggregates and metakaolin waste

was determined according to EN 12390-7 [20]. The specimen volume was calculated from the measured dimensions, and the mass was measured after oven drying at 40 ± 5 °C until a constant mass was achieved.

For each composition, at least three samples were tested, and the reported values represent the mean results. Standard deviations were calculated and are presented in the corresponding figures and tables.

The softening test was performed by immersing the specimens in water for 24 h. After water exposure, the samples were removed from the water, surface-dried, and immediately tested for compressive strength under the same testing conditions. The softening coefficient was calculated as the ratio between the compressive strength after water immersion and the compressive strength of the dry specimens, reflecting the reduction in mechanical performance caused by water saturation.

To determine the loss-on-ignition (LOI), the following method was employed. Firstly, 2 g of the material was calcined at 400 °C for 1.5 h. After that, the LOI value was calculated as the relative difference between the initial and final mass of the samples.

To assess the sound insulation properties of the composite samples, a dedicated acoustic testing case was employed. The tested panels had dimensions of 200 × 200 mm and a thickness of 180 mm. The samples were mounted between the sound source and receiving sections of the acoustic case, ensuring that sound transmission occurred only through the tested material. The setup consisted of a Visaton BG17 full-range loudspeaker (VISATON GmbH & Co. KG, Haan, Germany) mounted on one side of the enclosure and a microphone positioned on the opposite side, enabling controlled evaluation of sound transmission through the panel (Figure 3). A Vector Research VA-1400 amplifier (Vector Research, Chatsworth, CA, USA) supplied a stable acoustic signal.

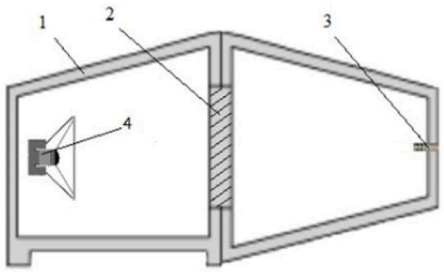


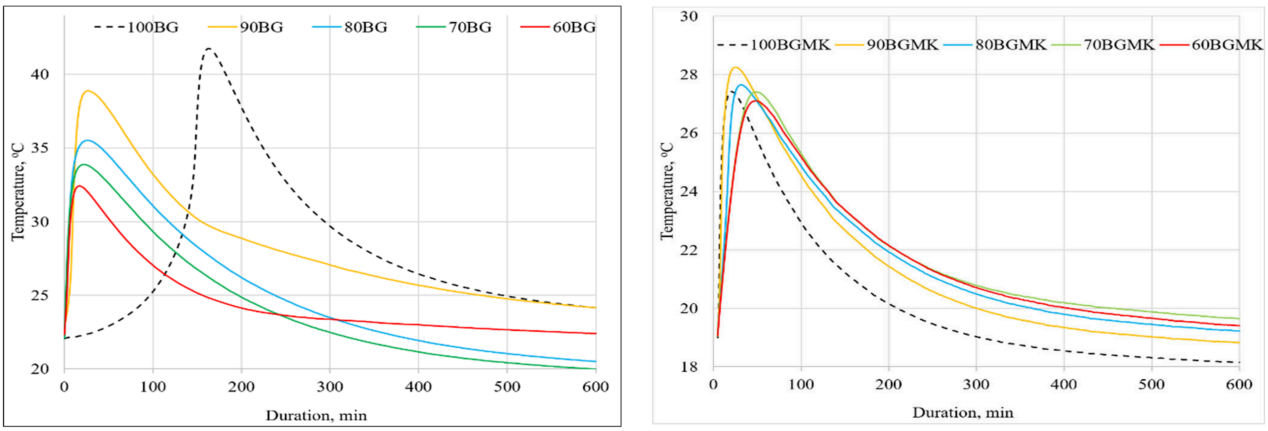
Figure 3. Scheme of the measuring stand. 1—Sound-insulating body of the stand; 2—Sample opening; 3—Microphone; 4—Noise source (loudspeaker).

Prior to testing, the measurement system was calibrated according to the equipment manufacturer's recommendations. The sound pressure level (SPL) was quantified using two complementary approaches: measurement of total noise levels and frequency spectrum analysis using standard octave-band filters (31.5, 63, 125, 250, 500, 1000, 2000, 4000, and 8000 Hz). For each composite composition, measurements were repeated three times and the reported values represent the average results. This methodology provided a comprehensive characterization of the composite's ability to attenuate sound across a broad frequency range. Acoustic insulation tests were carried out in accordance with the requirements of LST EN ISO 10140-2 [21].

3. Results and Discussion

At the initial stage, the hydration temperature was determined for samples without the metakaolin additive (Figure 4a). The reference mixture 100BG exhibits the highest hydration temperature, reaching 41.5 °C, which reflects the typical exothermic behavior of pure building gypsum during setting. This value is characteristic of systems in which

the hemihydrate content is the highest and the hydration reaction proceeds intensively, without the influence of modifying fillers. As the amount of RGPAs in the system increases, the hydration peak gradually decreases, and the maximum temperature becomes lower. This trend is particularly evident in the 60BG mixture, whose maximum hydration peak reaches only 32.4 °C. This reduction in temperature is directly related to the lower amount of active gypsum binder in the mixture: RGPAs, dominated by $CaSO_4 \cdot 2H_2O$, do not undergo the exothermic hemihydrate hydration reaction, and therefore the overall heat release is reduced.



(**a**) (**b**)

Figure 4. Hydration temperature of gypsum-based matrix composites: without metakaolin additive (**a**) and with metakaolin additive (**b**).

Changes in the duration of the hydration peaks also correlate with the RGPA content. As the proportion of RGPAs increases, the maximum hydration peak not only decreases in magnitude but also becomes shorter in duration. This phenomenon may be attributed to the presence of calcium sulphate dihydrate, as $CaSO_4 \cdot 2H_2O$ is known to promote crystal nucleation and shorten the period of intensive hydration. Consequently, mixtures with higher RGPA contents exhibit a faster but less exothermic hydration process. The incorporation of $CaSO_4 \cdot 2H_2O$ particles into a $CaSO_4 \cdot 0.5H_2O$ system is one of the most commonly used approaches for accelerating hemihydrate hydration and setting. Therefore, the accelerated hydration observed in RGPA-containing mixtures may be associated with gypsum dihydrate particles that provide additional nucleation surfaces for crystal growth. At the same time, RGPAs also contain residual paper fibres and other impurities originating from plasterboard waste, which may influence hydration kinetics and crystal development. However, further investigations would be required to confirm this mechanism directly.

In the presence of dihydrate, the dissolution of hemihydrate in the solution proceeds more intensively, as the supersaturation state is reached more rapidly, and Ca^{2+} and SO_4^{2-} ions can immediately precipitate onto existing crystalline surfaces. This observation aligns well with synchrotron-based kinetic studies [22], which show that adding more gypsum seeds increases the overall reaction rate. The seeds provide ready-made nucleation sites, so nucleation becomes much faster, and the hemihydrate begins transforming into dihydrate almost immediately. In other words, a higher amount of seeds directly accelerates the start of the reaction and significantly shortens the induction period. In contrast, the setting retarder TARDA (tartaric acid) prolonged the setting time of the gypsum paste. This observation is consistent with findings reported for tartaric acid in calcium sulphoaluminate systems, where tartaric acid significantly retards the hydration process, delaying the setting and reducing the early heat release [23]. In this case, the maximal hydration temperatures were reached after 28 min for the 90BG mixture and 20 min for the 60BG mixture, indicating

that the time required to reach the peak exothermic reaction decreased as the proportion of RGPAs increased. This behavior is consistent with the accelerating influence of dihydrate, which promotes rapid crystal formation and shortens the intensive hydration period.

Next, the hydration temperature was evaluated in mixtures where a metakaolin additive was incorporated into the gypsum matrix (Figure 4b). The introduction of metakaolin waste into the system significantly altered the hydration process by reducing the intensity of the exothermic reaction and slowing the temperature-rise dynamics compared to samples without MKW (Figure 4a). When comparing the samples with MKW, their hydration temperatures changed only slightly, ranging from 27.4 °C to 27.1 °C for the 100BGMK and 60BGMK mixtures, respectively. This difference indicates that metakaolin may act as a reactive micro-filler, may adsorb part of the water and reducing the exothermicity of hemihydrate hydration.

As the RGPA content increases in mixtures containing MKW, the hydration peak decreases slightly further. This shows that the effects of MKW and RGPAs on hydration are additive: both components reduce the exothermic reaction, while MKW also stabilizes the temperature-rise profile. The highest hydration temperature among MKW-containing mixtures was reached by the 90BGMK sample. This system exhibits an optimal hemihydrate-to-metakaolin ratio, resulting in the most intense exothermic reaction. The maximum hydration temperature in the 90BGMK mixture is reached after approximately 28 min, while in 60BGMK it occurs after about 20 min, reflecting the accelerating effect of dihydrate and the influence of metakaolin on hydration kinetics.

Changes in hydration-peak duration also correlate with the amounts of MKW and RGPAs. As the proportion of RGPAs increases, the duration of the hydration peak shortens (Figure 4a), but the presence of MKW partially compensates for this effect. Metakaolin slows the onset of crystal formation, causing the hydration peak to occur later and be less pronounced. This phenomenon is associated with metakaolin's ability to fill intercrystalline voids and adsorb part of the free water, thereby modifying hydration kinetics. As a result, in mixtures containing MKW, the hydration reaction becomes not only less exothermic but also more controlled.

Figure 5a illustrates how recycled gypsum plasterboard aggregates (RGPAs) and metakaolin waste (MKW) affect the mechanical performance and water resistance of gypsum-based matrix composites.

Before immersion, the samples without metakaolin (100–60BG) exhibit higher compressive strength compared to the mixtures containing MKW. The compressive strength of the 100BG mixture reaches approximately 22 MPa, and as the amount of recycled gypsum plasterboard aggregates (RGPAs) increases, the initial strength gradually decreases: 90BG—about 20 MPa, 80BG—18 MPa, 70BG—16 MPa, and 60BG—only about 14 MPa. This reduction may be attributed to the combined effects of a lower proportion of reactive hemihydrate, a higher content of inert RGPA particles, and the slight increase in the W/G ratio required to maintain normal consistency. The higher W/G ratio may contribute to increased porosity and consequently lower compressive strength.

Mixtures containing metakaolin waste (100—60BGMK) show slightly lower initial strength compared to mixtures without MKW. The compressive strength of 100BGMK reaches about 18 MPa, 90BGMK—17 MPa, 80BGMK—16 MPa, 70BGMK—15 MPa, and 60BGMK—approximately 14 MPa. This decrease is associated with metakaolin's ability to adsorb part of the water and act as a micro-filler, which modifies the early hydration environment and slows the onset of crystal growth. Nevertheless, the compressive strength values remain relatively stable across all MKW-containing mixtures, indicating that metakaolin does not disrupt matrix formation but only slightly adjusts its kinetics.

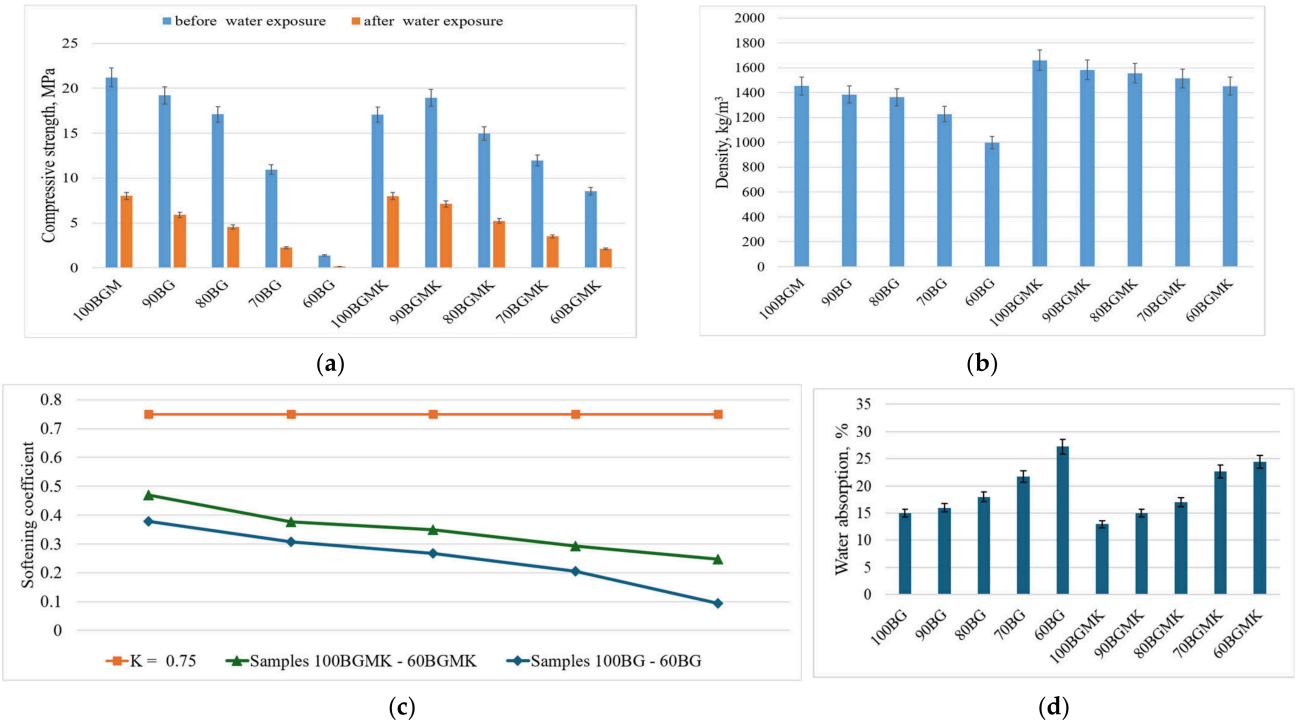


Figure 5. Influence of recycled gypsum plasterboard aggregates and metakaolin waste on the compressive strength (**a**), dry density (**b**), softening coefficient (**c**), and water absorption (**d**) of gypsum composites.

Figure 5b shows that the density of the samples follows similar compositional trends as compressive strength. Mixtures without metakaolin (BG series) exhibit lower densities, decreasing gradually with increasing RGPA content: 100BG reaches approximately 1453 kg/m^3 and 60BG—about 998 kg/m^3. This reduction may reflect both the increasing proportion of inert plasterboard particles and the higher W/G ratio, which may result in a less compact hardened matrix and increased water absorption.

In contrast, mixtures containing metakaolin waste (BGMK series) demonstrate consistently higher densities across all compositions. The density of 100BGMK reaches around 1661 kg/m^3 and 60BGMK—approximately 1452 kg/m^3. The higher density of MKW-modified samples could be indicated improved packing efficiency and matrix consolidation.

The softening coefficient indicates the proportion of the initial compressive strength that the mixtures retain after water exposure (Figure 5c). For reference, a threshold value of K = 0.75 is provided, below which the material is considered sensitive to moisture. In mixtures without metakaolin, the softening coefficient decreases sharply—from 0.38 (100BG) to only 0.09 (60BG). This pronounced reduction shows that, as the amount of RGPAs increases, the crystalline matrix becomes progressively less resistant to the dissolution of hydration products and structural degradation caused by water. In mixtures containing metakaolin waste, the softening coefficient remains significantly higher—ranging from 0.47 (100BGMK) to 0.25 (60BGMK). This demonstrates that metakaolin enhances matrix stability under wet conditions by reducing the loss of soluble phases and limiting water-induced structural deterioration. In similar research studies, the addition of MK increased the durability of gypsum composites, which is consistent with the findings reported by Yildizel [13], who demonstrated that metakaolin improves the mechanical performance and microstructural stability of gypsum-based composites reinforced with basalt fibers.

The water absorption results (Figure 5d) are consistent with the density measurements. For mixtures without metakaolin waste (BG series), water absorption increased progressively from approximately 15.0% for 100BG to 27.2% for 60BG. A similar trend was observed

for the BGMK series, where water absorption increased from about 13.2% for 100BGMK to 24.5% for 60BGMK. At all replacement levels, mixtures containing metakaolin waste exhibited lower water absorption than the corresponding BG mixtures. The reduction was particularly evident at higher RGPA contents. These results indicate that the incorporation of metakaolin waste contributes to a less permeable composite structure and reduces water uptake. Nevertheless, the observed behavior is influenced by the combined effects of RGPA content, metakaolin addition, and the corresponding variations in the water-to-gypsum ratio required to achieve normal consistency.

Figure 6a presents the XRD patterns of the BG-based composites (60BG and 100BG). Both diffractograms exhibit the characteristic reflections of gypsum dihydrate (G), confirming that $CaSO_4 \cdot 2H_2O$ remains the predominant crystalline phase after hardening. Minor peaks corresponding to dolomite (D) and quartz (Q) are also observed; these phases originate from the raw BG and RGPA materials and act as inert mineral fillers, contributing to the heterogeneity of the composite microstructure. Similar quartz- and carbonate-containing mineral phases have been identified in recycled gypsum composites and gypsum-based construction materials, where they were associated with impurities inherited from the original raw materials and recycled fractions [23,24].

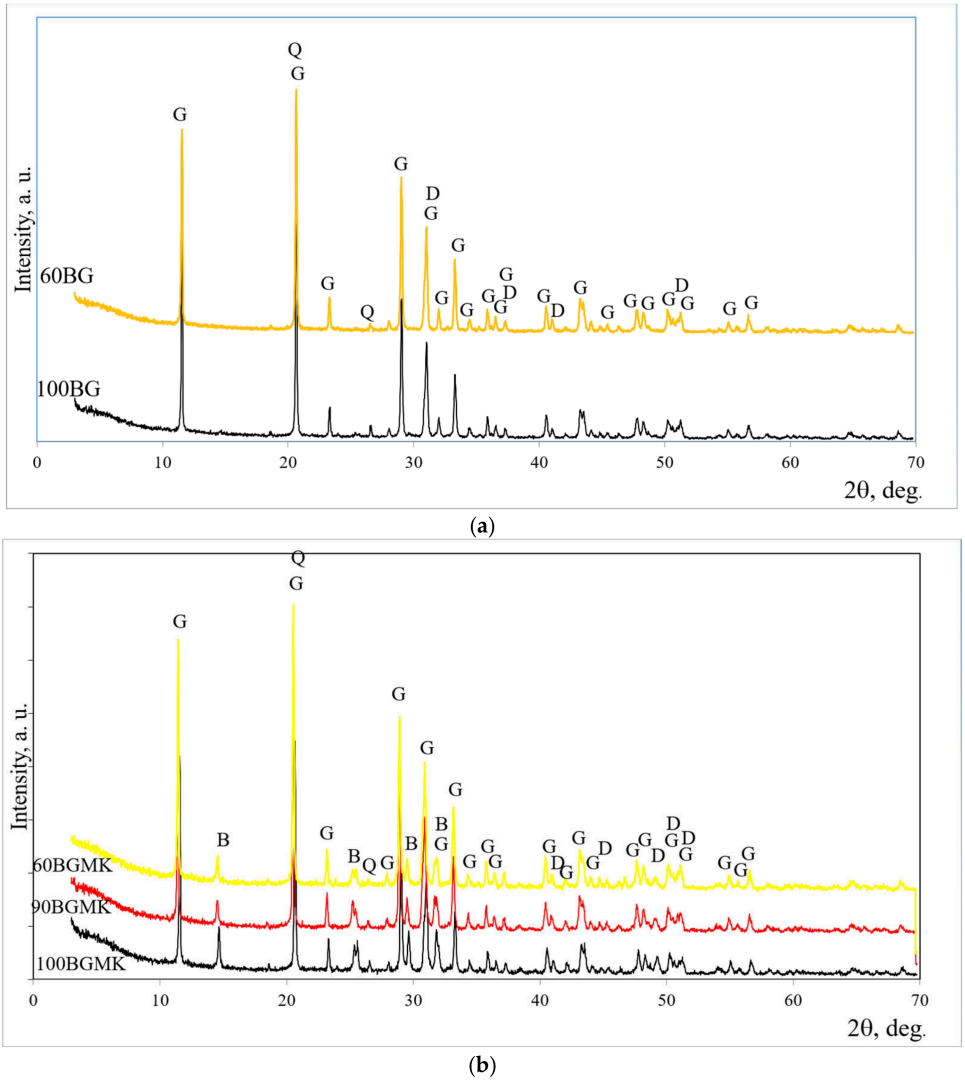


Figure 6. Mineral composition (XRD analysis) of gypsum-based matrix composites without MKW (**a**) and with MKW (**b**). Notes: G—gypsum $CaSO_4 \cdot 2H_2O$ (33–331), B—basanite $CaSO_4 \cdot 0.5H_2O$ (33–310), D—dolomite $CaMg(CO_3)_2$ (74–1687), Q—quartz SiO_2 (72–916).

In the BGMK series, samples (Figure 6b) show the XRD results (60BGMK, 90BGMK, and 100BGMK). Similar to the BG samples, all samples are dominated by gypsum dihydrate (G). In addition, low-intensity peaks of dolomite (D), quartz (Q) and traces of bassanite (B) are detected. The presence of residual bassanite may indicate a less complete conversion of hemihydrate to gypsum dihydrate during hydration.

This behaviour is consistent with metakaolin-modified systems, where metakaolin slows down hydration kinetics through water adsorption and altered dissolution–precipitation dynamics, resulting in delayed phase transformation [25,26]. It can be assumed that the presence of metakaolin waste slows down the hydration process, resulting in the incomplete conversion of bassanite to gypsum dihydrate.

Figure 7 presents SEM micrographs of gypsum-based matrix composites formulated according to Table 1, comparing mixtures without metakaolin waste (100BG), mixtures containing 10 wt.% metakaolin waste (100BGMK), and composites containing both metakaolin waste and recycled gypsum plasterboard aggregates (90BGMK).

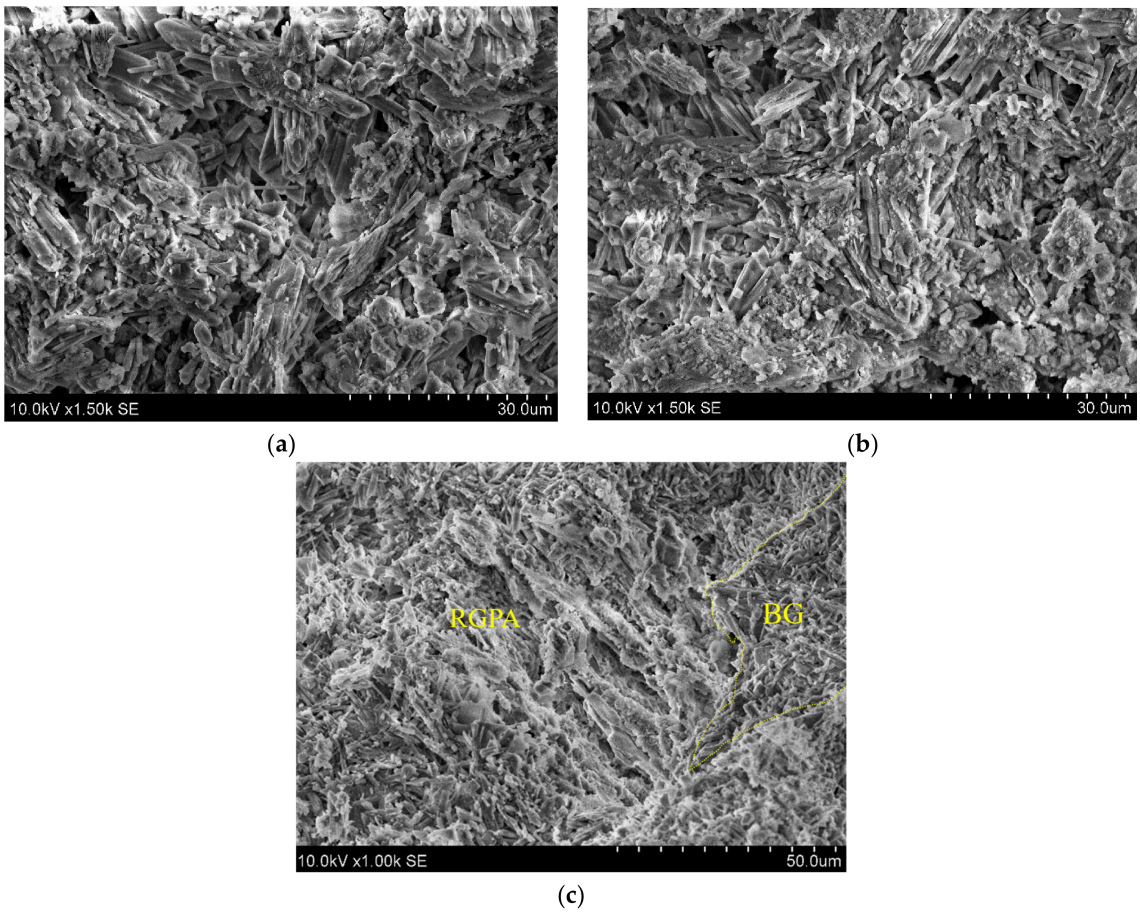


Figure 7. SEM images of gypsum-based matrix composites: without metakaolin additive 100BG (**a**), with metakaolin additive 100BGMK (**b**) and with metakaolin and BG additives 90BGMK (**c**).

The 100BG sample (Figure 7a) exhibits a microstructure dominated by elongated acicular gypsum dihydrate crystals, forming an open, interlocking network. Several pore clusters are also visible, reflecting the relatively high W/G ratio and the absence of microstructural modifiers. This morphology is consistent with previous studies on gypsum-based materials, which reported that gypsum crystallizes as elongated needle-like crystals that interlock to form a porous microstructure, with pore development being strongly affected by the water-to-gypsum ratio [26,27]. The SEM observations are supported by XRD results presented

in Figure 5. In 100BG, the diffractograms show that gypsum dihydrate (G) remains the predominant crystalline phase after hardening [28].

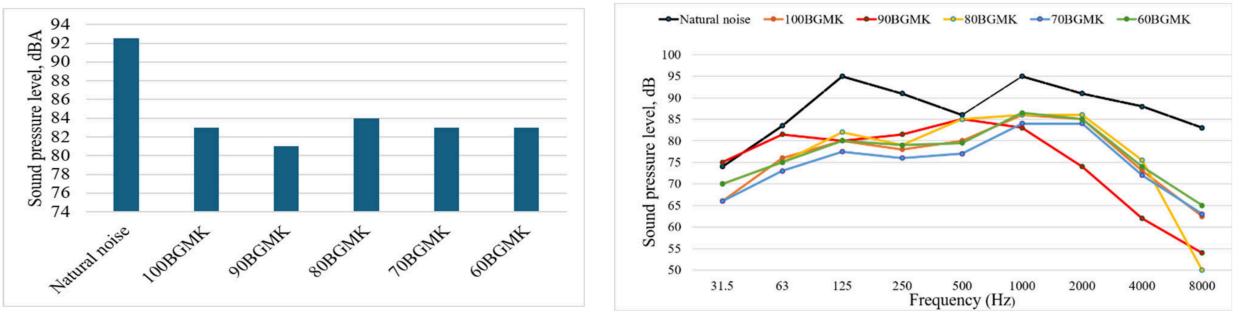
In contrast, the 100BGMK (Figure 7b) demonstrates significantly denser and more refined microstructures. Gypsum crystals appear shorter, thicker, and more tightly intergrown, indicating modified nucleation and growth behaviour in the presence of metakaolin waste. MKW acts as a reactive micro-filler, providing additional nucleation surfaces and adsorbing part of the free water, which limits excessive crystal elongation. Similar observations have been reported in cementitious systems, where metakaolin acts as a reactive micro-filler, providing additional nucleation sites and adsorbing free water, thereby refining crystal morphology and limiting excessive crystal elongation [23]. In another study [29], it was stated that metakaolin-containing gypsum systems exhibit modified hydration pathways and microstructural development due to the interaction between metakaolin particles, lime, and gypsum, influencing nucleation and phase formation. In this case, gypsum dihydrate (G) also dominates the phase composition (XRD analysis). However, low-intensity reflections of bassanite (B) are detected, indicating incomplete conversion of hemihydrate during hydration. The presence of MKW slows down the hydration process, likely due to water adsorption and altered dissolution–precipitation dynamics, resulting in partial retention of bassanite.

For the samples with metakaolin and RGPA additives (90BGMK) (Figure 7c), RGPA particles appear as irregular dihydrate fragments embedded within the matrix, locally disrupting crystal continuity and increasing pore concentration. As RGPAs are included in the system, the microstructure becomes progressively more heterogeneous, with lower density, larger pore clusters, and reduced crystal packing density. This behaviour is consistent with the higher W/G ratios (0.41–0.42) and the inert nature of RGPAs, which does not participate in hemihydrate hydration. These observations suggest that MKW still contributes to local microstructural refinement, but its stabilizing effect is partially diminished in the presence of RGPAs.

The sound pressure level measurements presented in Figure 8 enable the assessment of the acoustic response of different composite materials across the entirely investigated frequency range. Initially, the natural background noise generated in the testing stand was evaluated. The measured sound pressure level of 92.5 dBA exceeded the permissible 8 h exposure limit of 87 dBA (Figure 8a). To reduce noise, partition panels manufactured from BG, RGPAs, and MKW composites (their composition is provided in Table 2) were employed. All gypsum-based composite partitions demonstrated a comparable reduction in sound level, lowering it to 84–82 dBA. Based on the data illustrated in the graph, it can be concluded that all investigated composites contributed to noise reduction relative to the natural background noise; however, the highest overall noise attenuation efficiency was achieved by the 90BGMK specimen, which exhibited the lowest A-weighted sound pressure level of 82 dBA. Similar approaches have been reported in studies by Selvaraj et al. [30], who demonstrated that gypsum-based composites incorporating porous recycled materials can effectively reduce sound pressure levels across a wide frequency range. Their findings support the assumption that pore-forming additives improve acoustic damping performance, which is also relevant for the composites investigated in this work.

After evaluating the performance of the samples across different frequencies, it was determined that all tested specimens reduced the noise level, although the effectiveness depended on the sound wave frequency (Figure 8b). In the BG system, the decrease in base gypsum (BG) and the corresponding increase in recycled gypsum plasterboard aggregates (RGPAs) result in a systematic reduction in the sound pressure level, particularly at higher frequencies. This behavior may be associated with increased porosity and heterogeneity, which intensify sound attenuation in the mid- and high-frequency ranges. The sound

pressure levels of all samples at low frequencies (31.5–250 Hz) are positioned relatively close to each other. This indicates that the transmission of low-frequency waves is less dependent on the composition and microstructure. Such a trend is typical for mineral matrices, where low-frequency attenuation is limited due to the longer wavelengths and lower sensitivity to changes in porosity, a phenomenon also highlighted in recent acoustic studies of porous materials, which report that low-frequency absorption remains weak and only minimally influenced by pore structure variations [31].



(**a**) (**b**)

Figure 8. Dependence of the sound pressure level of natural noise on the amount of recycled gypsum plasterboard aggregates waste in gypsum composite at a standard octave frequency (**a**,**b**).

As the frequency increases (mid-frequency range, 250–2000 Hz), the influence of sample composition on the acoustic response becomes more pronounced. Mixtures with higher RGPA content (e.g., 70BG, 60BG) exhibit a consistent decrease in sound pressure level. RGPA particles create a more heterogeneous matrix, which more effectively attenuates mid-frequency waves [32].

In the high-frequency range (2000–8000 Hz), only minor differences emerge between the tested samples, which is typical for acoustic studies involving porous mineral matrices. The compositions containing RGPAs exhibit a consistent attenuation trend; however, the most pronounced effect is observed in the 90BGMK specimen, where the curve shows a sharp drop above 4000 Hz. This behavior is characteristic of composites in which microstructural heterogeneity induces intense scattering of high-frequency sound waves. This behavior is consistent with observations reported for porous polycrystalline materials, where microstructural heterogeneity significantly enhances the scattering of high-frequency acoustic and ultrasonic waves [33].

Overall, the results demonstrate that gypsum-based composites—particularly those modified with metakaolin waste and RGPA—provide effective broadband noise attenuation, with their performance governed by microstructural heterogeneity and its influence on sound scattering across different frequency ranges.

It should be noted that only one metakaolin waste dosage (10 wt.%) was investigated in this study. Therefore, although the results demonstrate the beneficial effect of MKW on the performance of gypsum composites, the optimum MKW content remains to be established and should be addressed in future studies employing a broader experimental design.

4. Conclusions

- Hydration temperature measurements showed that both RGPAs and MKW substantially modified the thermal behaviour of gypsum-based composites by reducing the maximum exothermic peak temperature. RGPAs shorten the peak duration by accelerating dihydrate-induced nucleation, whereas metakaolin waste prolongs it by increasing water adsorption and delaying crystal formation, resulting in a more gradual temperature development during hydration.

- The combined analysis of compressive strength and softening coefficient reveals a clear trend: mixtures containing metakaolin waste retain a larger portion of their initial strength after water exposure, whereas mixtures without MKW undergo more severe degradation. The incorporation of metakaolin waste increased the softening coefficient by 0.09 (from 0.38 to 0.47) in the 100BG mixture and by 0.16 (from 0.09 to 0.25) in the 60BG mixture. The results suggest that MKW may contribute to improved moisture resistance; however, the observed softening coefficients reflect the combined effects of MKW incorporation, RGPA content, and slightly variations in the W/G ratio rather than the influence of a single factor.
- XRD analysis shows that gypsum dihydrate is the main crystalline phase in all BG and BGMK composites, while dolomite and quartz act as inert fillers. In the BGMK samples, residual bassanite indicates slowed hydration, leading to the incomplete conversion of hemihydrate to dihydrate.
- SEM analysis shows that metakaolin waste promotes microstructural densification by producing shorter, thicker, and more intergrown gypsum crystals, whereas RGPAs disrupt this refinement, increasing porosity and reducing crystal packing. As a result, MKW enhances microstructural stability, but its beneficial effect is partially diminished when RGPAs are incorporated into the composite.
- The acoustic properties directly depend on composite composition and microstructural changes. The acoustic performance of sustainable gypsum composites can be deliberately modified by adjusting the amount of RGPAs. The 90BGMK samples demonstrated the highest efficiency, achieving the lowest sound pressure level (82 dBA) and providing the strongest attenuation of high-frequency noise. The 70BGMK and 60BGMK mixtures showed more uniform damping, across the entire frequency range. In summary, all specimens reduced noise by approximately 8.5–10.5 dBA compared to natural background noise.

Overall, metakaolin waste acts as an effective microstructural stabilizer in gypsum-based composites containing recycled gypsum plasterboard aggregates. MKW appears to partially compensate for the heterogeneity introduced by RGPAs, as indicated by the observed microstructural results. Considering hydration behavior, mechanical performance, microstructure, and acoustic properties together, no single mixture can be defined as fully optimal because the results are affected by both RGPA content and the corresponding variations in the W/G ratio necessary to maintain normal consistency. Consequently, the observed trends reflect the combined influence of these factors rather than the effect of any single variable.

Within the scope of this study, mixtures with intermediate RGPA content (such as 70BGMK) provide the most balanced combination of properties.

Author Contributions: Conceptualization, D.V. and V.V.; methodology, D.N.; software, J.M. and V.V.; validation, D.V., V.V. and L.V.; formal analysis, V.V.; investigation, D.N. and J.M.; resources, L.V.; data curation, D.V. and L.V.; writing—original draft preparation, D.V.; writing—review and editing, D.N. and J.M.; visualization, D.N.; supervision, D.V.; funding acquisition, J.M. and L.V. All authors have read and agreed to the published version of the manuscript.

Funding: This project has received funding from the Research Council of Lithuania (LMTLT), agreement No [S-PD-24-125].

Data Availability Statement: The original contributions presented in this study are included in the article. Further inquiries can be directed to the corresponding author.

Conflicts of Interest: The authors declare no conflicts of interest.

References

1. Weimann, K.; Adam, C.; Buchert, M.; Sutter, J. Environmental evaluation of gypsum plasterboard recycling. *Minerals* **2021**, *11*, 101. [CrossRef]
2. Erbs, A.; Nagalli, A.; de Carvalho, K.Q.; Mazer, W.; de Moraes Erbs, M.; Paz, D.H.; Lafayette, K.P. Development of plasterboard sheets exclusively from waste. *J. Build. Eng.* **2021**, *44*, 102524. [CrossRef]
3. Pérez-Galvez, F.; Pedreño-Rojas, M.A.; Morales-Conde, M.J.; Romero-Gómez, M.I.; Rubio-de Hita, P. Gypsum plasterboard waste as a raw material for the production of new eco-friendly plaster composites: The case of the Spanish industry. *Results Eng.* **2025**, *27*, 106097. [CrossRef]
4. Ma, X.; Tan, L.; Lu, Y.; Yao, W.; Wei, Y. Upcycling of waste plasterboard for the synthesis of high-quality gypsum-based 3D printing powder. *Constr. Build. Mater.* **2023**, *373*, 130846. [CrossRef]
5. Geraldo, R.H.; Pinheiro, S.M.; Silva, J.S.; Andrade, H.M.; Dweck, J.; Gonçalves, J.P.; Camarini, G. Gypsum plaster waste recycling: A potential environmental and industrial solution. *J. Clean. Prod.* **2017**, *164*, 288–300. [CrossRef]
6. Petropavlovskaya, V.; Buryanov, A.; Novichenkova, T.; Petropavlovskii, K. Gypsum composites reinforcement. In *IOP Conference Series: Materials Science and Engineering*; IOP Publishing: Bristol, UK, 2018; Volume 365, p. 032060.
7. Vimmrova, A.; Keppert, M.; Svoboda, L.; Černý, R. Lightweight gypsum composites: Design strategies for multi-functionality. *Cem. Concr. Compos.* **2011**, *33*, 84–89. [CrossRef]
8. Doleželová, M.; Scheinherrova, L.; Krejsová, J.; Keppert, M.; Černý, R.; Vimmrova, A. Investigation of gypsum composites with different lightweight fillers. *Constr. Build. Mater.* **2021**, *297*, 123791. [CrossRef]
9. Balti, S.; Boudenne, A.; Yahya, K.; Hamdi, N. Advancing reinforcement of sustainable gypsum composites: High-performance design by reusing waste materials. *Mater. Today Sustain.* **2024**, *27*, 100946. [CrossRef]
10. Wang, S.; Pancheti, J.; Xi, Y.; Mahendran, M. Lightweight composite gypsum boards with clay mineral and glass fibre for enhanced fire-resistance. *Compos. Part B Eng.* **2023**, *266*, 111044. [CrossRef]
11. Argalis, P.P.; Bumanis, G.; Bajare, D. Gypsum composites with modified waste expanded polystyrene. *J. Compos. Sci.* **2023**, *7*, 203. [CrossRef]
12. Kishor, C.; Chawla, H. Synergistic effect of metakolin, flue gas desulfurization gypsum and glass cullets in the development of sustainable mortar. *Sustain. Chem. Pharm.* **2026**, *52*, 102442. [CrossRef]
13. Yildizel, S.A. Material properties of basalt-fiber-reinforced gypsum-based composites made with metakaolin and silica sand. *Mech. Compos. Mater.* **2020**, *56*, 379–388. [CrossRef]
14. Moradi, H.; Azima, S.; Ebrahimi-Kahrizsangi, R. Comparison and study of mechanical and physical properties of metakaolin reinforced gypsum composite. *Compos. Theory Pract.* **2023**, *23*, 129–135. [CrossRef]
15. Raja, M.A.; Sujatha, S.J.; Yadav, A.; Sophia, M. Design of an eco-friendly composite gypsum binder using different mineral admixtures. *Mater. Today Proc.* **2022**, *62*, 5519–5525. [CrossRef]
16. Fraire-Luna, P.E.; Escalante-Garcia, J.I.; Gorokhovsky, A. Composite systems fluorgypsum–blastfurnance slag–metakaolin, strength and microstructures. *Cem. Concr. Res.* **2006**, *36*, 1048–1055. [CrossRef]
17. *EN 196-9:2010*; Methods of Testing Cement. Heat of Hydration. Semi-Adiabatic Method. European Committee for Standardization (CEN): Brussels, Belgium, 2010.
18. *EN 196-3*; Methods of Testing Cement—Part 3: Determination of Setting Times and Soundness. CEN/TC 51 Cement and Building Limes. European Committee for Standardization: Brussels, Belgium, 2016.
19. *EN 13279-2:2014*; Gypsum Binders and Gypsum Plasters—Part 2: Test Methods. European Committee for Standardization: Brussels, Belgium, 2014.
20. *EN 12390–7*; Testing Hardened Concrete—Part 7: Density of Hardened Concrete. European Committee for Standardization: Brussels, Belgium, 2019.
21. *LST EN ISO 10140-2:2021*; Acoustics—Laboratory Measurement of Sound Insulation of Building Elements—Part 2: Measurement of Airborne Sound Insulation. Lithuanian Standards Board: Vilnius, Lithuania, 2021.
22. Gurgul, S.J.; Seng, G.; Williams, G.R. A kinetic and mechanistic study into the transformation of calcium sulfate hemihydrate to dihydrate. *Synchrotron Radiat.* **2019**, *26*, 774–784. [CrossRef]
23. Jing, H.; Li, M.; Zhang, Y.; Gao, M. Hydration kinetics, microstructure and physicochemical performance of metakaolin-blended cementitious composites. *Constr. Build. Mater.* **2023**, *408*, 133756. [CrossRef]
24. Chandara, C.; Azizli, K.A.M.; Ahmad, Z.A.; Sakai, E. Use of waste gypsum to replace natural gypsum as set retarders in portland cement. *Waste Manag.* **2009**, *29*, 1675–1679. [CrossRef]
25. Cordon, H.C.F.; Ferreira, M.S.; Ferreira, F.F. Comparative analysis of recycled plaster composition determined by X-ray powder diffraction and thermogravimetric analyses. *Constr. Mater.* **2021**, *1*, 105–121. [CrossRef]
26. Zhan, P.; Sun, X.; Wang, D.; Wang, D.; Lin, W.; Lin, X.; Wang, J.; Tam, V.W. Synergistic effects of metakaolin and limestone on early hydration kinetics, strength development, and microstructure of low water-to-binder ratio cement composites. *Case Stud. Constr. Mater.* **2026**, *24*, e06210. [CrossRef]

27. Kakar, F.M.; Pourattar, P.; Pritzel, C.; Kowald, T.; Killian, M.S. Supersaturation-Pathway-Controlled Gypsum Crystallization and Morphology: Nucleation-vs. Growth-Dominated Regimes with a Polycarboxylate Superplasticizer. *Crystals* **2026**, *16*, 241. [CrossRef]
28. Gordina, A.F.; Polianskikh, I.S.; Gumenuk, A.N.; Plekhanova, T.A. Examination of New Growths in Modified Sulfate-Based Composites by Scanning Electron Microscopy. *Crystallogr. Rep.* **2023**, *68*, 581–587. [CrossRef]
29. Žemlička, M.; Kuzielová, E.; Kuliffayova, M.; Tkacz, J.; Palou, M.T. Study of hydration products in the model systems metakaolin–lime and metakaolin–lime–gypsum. *Ceram. Silik.* **2015**, *59*, 283–291.
30. Selvaraj, V.K.; Subramanian, J.; Dutt, S.S.; Annamalai, K.; Natarajan, E.; Kumaresan, S. A comparative study on acoustical properties using waste recycled porous materials for environmental sustainability. *Sci. Rep.* **2025**, *15*, 26460. [CrossRef]
31. Suo, H.; Xu, J.; Feng, Y.; Liu, D.; Tang, P.; Feng, Y. Experimental Research and Theoretical Analysis of the Coupling Mechanism Between Microstructure and Acoustics in Porous Materials. *Appl. Sci.* **2025**, *15*, 3104. [CrossRef]
32. Hou, Z.; Zhou, Z.; Zhang, K.; Ji, Y.; Pan, L.; Zheng, Y.; Wang, L. Noise Reduction Characteristics of Porous Composite Acoustic Absorbers with Graded Adjustable Pore Structure. *SSRN* **2025**. [CrossRef]
33. Guo, Z.; Song, Y.; Li, X. Decoupling analysis of ultrasonic scattering characteristics in porous polycrystalline materials using phase field and finite element methods. *Ultrasonics* **2025**, *159*, 107864. [CrossRef]

Disclaimer/Publisher's Note: The statements, opinions and data contained in all publications are solely those of the individual author(s) and contributor(s) and not of MDPI and/or the editor(s). MDPI and/or the editor(s) disclaim responsibility for any injury to people or property resulting from any ideas, methods, instructions or products referred to in the content.